

GLOBAL INVERSION OF PHASE AND GROUP VELOCITIES OF FUNDAMENTAL MODE RAYLEIGH WAVES IN THE PERIOD RANGE 20 TO 100 SEC

João Willy Correa Rosa^{1*} & Keiiti Aki²

We have applied to the extensive phase and group velocity data compiled in a first stage of this work (Rosa, 1986; Rosa & Aki, 1991) the stochastic inverse method in order to obtain the global distribution of Rayleigh wave phase velocity values. This is the first attempt to invert globally a data set consisting entirely of R_1 , which does not suffer from polar passages which tend to complicate the waveform by multipath interferences. The resultant anomalies of the phase velocity correlate well with major tectonic features and with previous regional studies made for similar periods. It was demonstrated that these results at relatively longer periods can now be used for determining the moment tensor of events in most regions around the globe. Shorter period results, however, cannot be used in this fashion, due to large residual data variance. In the case of our group velocity study, we found that since the standard deviation of the regionalized values were very similar to those obtained in the phase velocity regionalization (Rosa, 1986; Rosa & Aki, 1991), the large, unacceptable error bounds achieved after the application of the stochastic inversion to the group velocity data, are related to the larger errors involved in the measurement of group velocity. This makes it much harder to obtain geophysical meaningful results from group velocity data.

INVERSÃO GLOBAL DE VELOCIDADES DE FASE E DE GRUPO DE ONDAS RAYLEIGH, NO MODO FUNDAMENTAL, COM PERÍODO ENTRE 20 E 100 SEGUNDOS – O método de inversão estocástica foi aplicado ao grande banco de dados de velocidade de fase e de grupo, de ondas Rayleigh no modo fundamental, com valores de período variando entre 20 e 100 segundos, coletado na primeira parte desta pesquisa (Rosa, 1986; Rosa & Aki, 1991). O objetivo do processo de inversão era a obtenção da distribuição global de valores de velocidade de fase. Neste sentido, nosso trabalho representa a primeira tentativa de obtenção de um modelo global deste tipo baseado apenas em dados de ondas R_1 , que não sofrem passagens pelos polos do percurso, o que normalmente tende a complicar os resultados, devido a efeitos de interferência na propagação das ondas. As anomalias de velocidade de fase obtidas no processo de inversão correlacionam-se bem com as principais feições tectônicas conhecidas na Terra e confirmam os resultados de estudos similares realizados em algumas das faixas de período estudadas. Demonstra-se aqui que os resultados nas faixas superiores do intervalo de período estudado podem agora ser usados para a determinação do tensor de momento de eventos localizados na maior parte do globo. Por outro lado, resultados para as faixas inferiores do intervalo de período estudado não podem ser usados para os mesmos objetivos, devido à grande variância residual associada aos resultados destas faixas. No caso do mesmo estudo realizado com os dados de velocidade de grupo, concluímos que, como o “standard deviation” dos valores regionalizados é similar ao dos valores regionalizados de velocidade de fase (Ro-

1. Department of Earth, Atmospheric and Planetary Sciences, Massachusetts Institute of Technology, Cambridge, MA 02139, USA

2. Department of Geological Sciences, University of Southern California, Los Angeles, CA 90089-0740, USA

* Present address: Instituto de Geociências, Departamento de Geologia Geral e Aplicada, Universidade de Brasília, 70910 Brasília, DF

sa, 1986; Rosa & Aki, 1991), os valores elevados e inaceitáveis de erros associados aos resultados do processo de inversão estocástica dos dados de velocidade de grupo, estão ligados aos grandes erros envolvidos na medida desta grandeza, se compararmos este processo às medidas de velocidade de fase. Assim, é muito mais difícil, em geofísica, obter resultados precisos em estudos de velocidade de grupo de ondas superficiais, do que em estudos da velocidade de fase destas ondas.

INTRODUCTION

In the first part of our work on fundamental mode Rayleigh waves in the period range 20 to 100 seconds (Rosa, 1986; Rosa & Aki, 1991), we compiled worldwide data of phase and group velocity measurements. We formed this data set using phase velocity from the existing literature, and by newly made phase and group velocity measurements for paths from a set of 45 globally distributed earthquakes with well known focal mechanism and depth to W.W.S.S.N. stations. These data were used to establish a set of regionalized phase and group velocity global models for these waves. We have now an extensive data set and initial models for both phase velocity and group velocity, which enable us to use linearized inversion scheme in order to determine the lateral distribution of phase velocity and group velocity.

Global studies on surface waves have, until now, been restricted to longer periods, which can be done using data from existing digital seismograph stations: I.D.A. and G.D.S.N., which includes S.R.O., A.S.R.O. and D.W.W.S.S.N.. This task has been pursued by two research groups, one at the California Institute of Technology (Nakanishi & Anderson, 1982, 1983, 1984a, b; Tanimoto & Anderson, 1984, 1985 and Tanimoto, 1985) and the other at Harvard University (Woodhouse & Dziewonski, 1984). The period range covered by such studies, as well as the source and amount of data used, are summarized in Tab. 1, and compared with those of our studies. Notice that our data set is much larger than others.

It is important to stress the fact that the work presented here is the first attempt to invert globally a data set consisting entirely of R_1 , which do not suffer from polar passages which tend to complicate the waveform by multipath interferences. Furthermore, the R_1 data set does not suffer from the non-uniqueness of the great circle phase velocity data (e.g. Nakanishi & Anderson, 1983), which cannot fully describe the Earth's lateral heterogeneity.

INVERSION METHOD

The stochastic inverse for linear problems was introduced by Franklin (1970) and first used by Jordan

(1972) in seismology. It was then used by Aki et al. (1977) for determination of the three-dimensional velocity distribution underneath a seismic network using the travel time data observed for teleseismic events. This method has been further extended to the inversion of local earthquake travel time data by Aki & Lee (1976). Since then, it has been improved and widely used in various areas (see reviews by Aki, 1977, 1979, 1981, 1982). In order to eliminate nonuniqueness of the solution Jackson (1979) included a priori information about the solutions in the formulation of the problem. More recently, Tarantola & Valette (1982) considered the stochastic inversion of data for nonlinear problems.

In this work, we apply the stochastic inverse to our dataset in order to determine the worldwide distribution of phase and group velocity of fundamental mode Rayleigh waves for the 20 to 100 sec period range.

We shall first describe the inversion method, comment on the analysis of error, and discuss the appropriate choice for the damping constant. The effect of the damping constant used in the stochastic inversion is discussed in terms of the assumed a priori model variance. In this discussion, we shall make use of abundant examples of three-dimensional inversion of body wave travel time data, in order to arrive at the appropriate damping constant.

We follow the inversion procedure using a block model introduced by Aki et al. (1977). Assuming ray theory, the phase arrival time t^c for a path between two points x_1 and x_2 can be calculated in terms of the phase velocity $c(x)$ at a point x along the path as

$$t^c = \int_{x_1}^{x_2} dx/c(x) \quad (1)$$

where dx is the incremental path length.

Let us designate the observed phase arrival time for the i -th path as t_i^o , and the calculated arrival time for the initial model t_i^c . We shall use the phase and group velocity models of Rosa & Aki (1991) based on Jordan's (1981) regionalized model with block size of 10° by 10° as our initial model. The residual travel time Δt_i is then defined as

$$\Delta t_i = t_i^o - t_i^c \quad (2)$$

Table 1. Some recent studies on global distribution of phase and group velocity of surface waves.

Reference	Period range (sec)	Type of study	Number of paths	Recording network
Nakanishi & Anderson (1982)	152-252	Rayleigh wave group velocity	215	I.D.A.
Nakanishi & Anderson (1983)	100-330	Love wave	200	I.D.A.
		Rayleigh wave phase velocity	250	G.D.S.N.
Nakanishi & Anderson (1984a,b) also	100-330	Love wave	408	I.D.A.
		Rayleigh wave group velocity	399	G.D.S.N.
Tanimoto & Anderson (1984, 1985) and Tanimoto (1985)		Love wave	289	
		Rayleigh wave phase velocity	414	
Woodhouse & Dziewonski (1984)	greater than 135 sec	Love and Rayleigh as well as body waveform data	870	I.D.A. G.D.S.N.
This work	20-100	Rayleigh wave phase velocity	2147	W.W.S.S.N.

We attribute the cause of these travel time residuals to the perturbation in velocity along the path. Dividing the Earth's surface into blocks, we can write

$$\Delta t_i = \sum_j g_{ij} m_j + e_i \tag{3}$$

where g_{ij} is the time spent by the i -th ray path in the j -th block, and m_j is the fractional slowness perturbation for this block. Since ray theory was used to define eq. (3), the block size is constrained by the wavelength of the seismic waves used. g_{ij} is obtained by calculating the length of the ray in each block and the velocity value assigned to the region to which the block belongs. e_i represents the errors due to measurement errors and higher order terms neglected in the linearization of the problem.

$$d = Gm + n \tag{4}$$

In matrix form, eq. (3) can be written as where d is a vector containing the residual time Δt_i observed

for the i -th path, G is a matrix with elements g_{ij} , m is the vector consisting of elements m_j , and n is the error vector with elements e_i . To obtain the stochastic inverse operator L , following the notation of Aki & Richards (1980), we assume that both m and n are stochastic processes, with zero mean ($\langle m \rangle = \langle n \rangle = 0$), and define their covariance matrices by

$$\langle mm^t \rangle = R_{mm}$$

$$\langle nn^t \rangle = R_{nn}$$

where the suffix t means taking the transpose of a matrix.

An inverse operator L is then calculated in a way that the averaged differences between m and Ld are minimized in the least squares sense.

$$L = (G^t R_{nn}^{-1} G + R_{mm}^{-1})^{-1} G^t R_{nn}^{-1} \tag{5}$$

This form is convenient to use in this problem, where

the data set is larger than the set of model parameters.

Aki et al. (1977) assume that

$$R_{nn} = \sigma_n^2 I \quad (6)$$

and

$$R_{mm} = \sigma_m^2 I \quad (7)$$

Equation (6) means that the measurement errors are independent and share the common variance and eq. (7) implies that all the parameters to be determined share the same model variance σ_m^2 ; and they are all statistically independent.

Using eqs. (6) and (7) in eq. (5) and introducing damping constant $\theta^2 = \sigma_n^2/\sigma_m^2$, we can rewrite

$$L = (G^t G + \theta^2 I)^{-1} G^t \quad (8)$$

so that the estimate m' of the solution is obtained by operating L on the data vector d ,

$$m' = L d \quad (9)$$

The resolution and the errors of the solution m' due to random noise in the data can be assessed (Backus & Gilbert, 1967, 1968, 1970) by checking the resolution and the covariance matrix:

$$R = L G \quad (10)$$

$$C = \sigma_n^2 L L^t \quad (11)$$

We can also define the covariance matrix that includes all the errors in the solution (Jackson, 1979)

$$\begin{aligned} \langle (m' - m)(m' - m)^t \rangle = \\ (R - I) \langle m m^t \rangle (R - I)^t + L \langle n n^t \rangle L^t \end{aligned} \quad (12)$$

For the special case $R_{nn} = \sigma_n^2 I$ and $R_{mm} = \sigma_m^2 I$, this simplifies to

$$\langle (m' - m)(m' - m)^t \rangle = \sigma_n^2 (G^t G + \theta^2 I)^{-1} \quad (13)$$

The best choice, according to the stochastic inverse, for the damping constant is given by $\theta^2 = \sigma_n^2/\sigma_m^2$. The error in the solution due to the linearization of the problem together with measurement errors have to be considered in the estimation of the noise variance σ_n^2 . This is estimated from the residual for the estimated solution m' .

$$e = d - G m'$$

and its magnitude

$$e^t e = d^t d - 2m'^t G^t d + m'^t G^t G m' \quad (14)$$

σ_n^2 is estimated by dividing $|e|^2$ by the number of degrees of freedom, that is, the number of data minus the number of model parameters, as done by Aki & Lee (1976) and Zandt (1978). On the other hand, σ_m^2 must be specified with an a priori assumption of the model. This introduces some subjectivity to the inversion process.

Table 2 shows the data variance, model variance and the damping constant used in several published three-dimensional inversion studies of travel time data for body-waves, using the method of Aki et al. (1977), along with the work of Biswas (written communication, 1983), who studied south-central Alaska using teleseismic data.

The damping constant θ^2 assumed by these authors are shown in Tab. 2. They are obtained by the relation $\theta^2 = \sigma_n^2/\sigma_m^2$ where σ_n^2 was, in some cases, estimated from the reading error in the measurements of arrival time, and σ_m was assumed by the author.

We were initially puzzled by a considerable discrepancy between the assumed value of σ_m and the root mean square of the solution, listed at the 6th and 7th lines of Tab. 2 for crust and mantle, respectively.

Examining the residual, $e = d - G m'$, we soon realized that some of the authors have underestimated σ_n^2 by considering only the reading error. The square root σ_n^* of the noise variance estimated from the residual is also listed in Tab. 2. The square root of the model variance corresponding to σ_n^* is calculated by the equation $\sigma_m = \theta^2/\sigma_n^{*2}$, and is listed at the 5th line of Tab. 2. Their values compare better with the root mean square of the solution.

An interesting feature of the inversion results may be observed in Tab. 2. It is clear that the velocity variations are greater in the crust than in the upper mantle, and that the velocity variations increase with the decrease in block size as shown in Tab. 2. As shown in Tab. 3 for other studies, the crust presents, in general, a velocity variation greater than the mantle. We list also in Tab. 4 the root mean square velocity variations, the average diagonal element of the resolution matrix and the average standard error of the solution due to random error in the data. The depth range, lateral block size and number of resolved blocks are also listed for each layer. It is clear from these results that there is a decrease of the velocity variation with depth.

The above review of the results of three-dimensional velocity studies using the stochastic inversion is useful in our application to Rayleigh waves, since it shows how to estimate the noise

Table 2

Ref.	Hirahara 1977	Hirahara 1981	Zandt 1978	Zandt 1978	Zandt 1978	Horie & Aki 1982	Taylor 1983	Biswas 1983
Region	Japan	Japan	Santa Rosa	San Jose	Bear Valley	Kanto District	Nevada	Alaska
θ^2 (sec/%) ²	0.15	0.10	0.005	0.005	0.005	0.01	0.01	0.005
Reading error (sec)	1.0	0.7	0.1	0.1	0.1	0.05	0.05	0.1
σ_m (%) assumed by author	2.58	2.21	1.41	1.41	1.41	0.50	0.50	1.41
σ_d^* from residual (sec)	0.78	1.01	0.14	0.26	0.14	0.20	0.34	0.36
σ_m from σ_d^* (%)	2.02	3.21	2.01	3.64	2.00	2.00	3.46	5.10
ΔV RMS crust (%)	1.96	2.40	2.92	3.24	3.00	3.50	3.17	4.16
ΔV RMS mantle (%)	1.45	1.57	2.71	1.90	2.26	1.35	2.54	1.80
Block size								
Max	2°	2°	25 km	25 km	25 km	30 km	20 km	100 km
Min	-	1°	10 km	10 km	10 km	-	10 km	65 km

where ΔV RMS = $\langle(\Delta V/V_0)^2\rangle^{1/2}$

Table 3

Reference	Region	ΔV RMS (%)		θ^2 (sec/%) ²	Block size (km)	
		Crust	Mantle		Max	Min
Aki et al., 1976	LASA, USA	1.29	0.82	0.02	20	-
Husebye et al., 1976	Central California	2.18	1.10	0.02	25	30
Aki et al., 1977	Norsar, Norway	1.20	1.20	0.02	20	-
Elisworth & Koyanagy, 1977	Hawaii	3.92	1.31	0.005	7.5	-
Mitchell et al., 1977	New Madrid, USA	1.78	1.45	0.02	50	-
Raikes, 1980	Southern California	2.34	1.71	0.01	40	55
Hasemi et al., 1984	Tohoku district, NE Japan	3.19	1.19	0.05	30	-

where ΔV RMS = $\langle(\Delta V/V_0)^2\rangle^{1/2}$

Table 4

Reference	Layer	RMS Vel Variations (%)	Average Resolution	Aver STD dev due to Random error (%)	Depth (km)	Block Size (km)	Resolved Blocks
Aki et al., 1976	1	1.45	0.56	-	0-20	20 x 20	23
	2	1.11	0.59	-	20-50	20 x 20	40
	3	0.91	0.52	-	50-80	20 x 20	60
	4	0.77	0.52	-	80-100	20 x 20	77
	5	0.77	0.59	-	110-140	20 x 20	79
Husebye et al., 1976	1	2.18	0.54	-	0-25	25 x 25	29
	2	1.14	0.40	-	25-50	25 x 25	35
	3	1.18	0.40	-	50-75	30 x 30	37
	4	1.00	0.37	-	75-100	30 x 30	48
	5	1.09	0.38	-	100-125	30 x 30	55
Aki et al., 1977	1	1.36	0.46	-	0-17	20 x 20	36
	2	1.02	0.40	-	17-36	20 x 20	48
	3	1.09	0.52	-	36-66	20 x 20	70
	4	1.09	0.51	-	66-96	20 x 20	80
	5	1.39	0.55	-	96-126	20 x 20	81
Hirahara, 1977	1	1.96	0.48	0.71	0-50	2° x 2°	31
	2	2.05	0.54	0.58	50-150	2° x 2°	40
	3	1.74	0.47	0.63	150-250	2° x 2°	39
	4	1.25	0.39	0.56	250-350	2° x 2°	43
	5	1.08	0.38	0.61	350-450	2° x 2°	47
	6	1.17	0.40	0.64	450-550	2° x 2°	54
	7	1.17	0.42	0.71	550-650	2° x 2°	61
Mitchell et al., 1977	1	2.05	0.37	0.25	0-20	50 x 50	15
	2	1.47	0.26	0.20	20-40	50 x 50	22
	3	1.34	0.65	0.24	40-97	50 x 50	33
	4	1.55	0.69	0.27	97-154	50 x 50	39
Zandt, 1978 Bear Valley	1	3.70	0.37	0.72	0-10	10 x 10	62
	2	2.06	0.57	0.70	10-30	20 x 20	43
	3	2.05	0.69	0.64	30-60	25 x 25	46
	4	2.44	0.66	0.69	60-90	25 x 25	53
Zandt, 1978 San Jose	1	4.02	0.43	1.45	0-10	10 x 10	63
	2	2.23	0.64	1.32	10-30	20 x 20	42
	3	2.05	0.75	1.12	30-60	25 x 25	45
	4	1.74	0.68	1.23	60-90	25 x 25	53
Zandt, 1978 Santa Rosa	1	2.57	0.27	0.70	0-10	10 x 10	39
	2	3.23	0.46	0.73	10-30	20 x 20	32
	3	3.08	0.65	0.66	30-60	25 x 25	33
	4	2.28	0.56	0.72	60-90	25 x 25	40

Table 4 (cont.)

Reference	Layer	RMS Vel Variations (%)	Average Resolution	Aver STD dev due to Random error (%)	Depth (km)	Block Size (km)	Resolved Blocks
Raikes, 1980	1	2.34	-	0.39	0-40	40 x 40	87
	2	1.57	-	0.40	40-100	45 x 45	99
	3	1.84	-	0.33	100-180	55 x 55	88
Hirahara, 1981	1	2.40	0.38	1.07	0-33	1 ^o x 1 ^o	79
	2	1.86	0.43	0.94	33-66	1 ^o x 1 ^o	98
	3	1.60	0.33	0.95	66-100	1 ^o x 1 ^o	101
	4	1.77	0.28	0.92	100-150	1 ^o x 1 ^o	105
	5	1.46	0.45	0.98	150-200	1 ^o x 1 ^o	98
	6	1.27	0.42	1.01	200-300	2 ^o x 2 ^o	27
	7	1.28	0.35	0.76	300-400	2 ^o x 2 ^o	27
	8	1.69	0.26	0.65	400-500	2 ^o x 2 ^o	14
	9	1.48	0.15	0.60	500-600	2 ^o x 2 ^o	8
Horie & Aki, 1982	1	3.50	0.56	0.77	0-32	30 x 30	34
	2	2.30	0.49	0.87	32-65	30 x 30	32
	3	1.08	0.37	0.90	65-98	30 x 30	24
	4	0.91	0.15	0.66	98-131	30 x 30	18
	5	0.21	0.02	0.27	131-164	30 x 30	4
Taylor, 1983	1	4.08	0.43	-	0-5	10 x 10	18
	2	2.69	0.55	-	5-17	10 x 10	35
	3	2.51	0.66	-	17-32	10 x 10	66
	4	2.06	0.67	-	32-70	10 x 10	67
	5	2.94	0.55	-	70-100	20 x 20	33
Hasemi et al., 1984	1	3.19	0.63	0.95	0-32	30 x 30	52
	2	1.54	0.67	0.93	32-65	30 x 30	56
	3	1.23	0.59	0.99	65-98	30 x 30	55
	4	1.66	0.41	0.99	98-131	30 x 30	49
	5	0.69	0.23	0.78	131-164	30 x 30	24
	6	0.18	0.04	0.47	164-197	30 x 30	4

variance, and how the lateral heterogeneities vary with depth. We have applied eq. (14) to estimate the noise variance in our data set, and found that different damping was needed while studying different periods, during the application of the stochastic inversion. We shall discuss the results of these analyses in the next sections.

APPLICATION OF THE STOCHASTIC INVERSION TO THE PHASE VELOCITY DATA

The operator L of eq. (8) was obtained for each

period, using the decomposition by the Cholesky algorithm (Strang, 1980). We have tried several damping constants for each period. In all cases, we required that each block was sampled by at least ten rays. In order to eliminate some anomalous observations, we rejected residual travel time data, with an absolute value more than four percent of the total travel time. For each run, corresponding to a given damping constant, we calculated the following parameters for each block: the number of hits in each block studied; the percentage velocity perturbation; the

Table 5

Period 20 sec. For this period: initial data variance = 683.8181 sec²; No. of observations = 751; No. blocks = 209; average path length = 5377.750 km.

Region	Number of blocks studied	RMS vel variations (%)	Average resolution	Aver total STD dev (%)	Aver STD dev due to Random error (%)	Aver STD dev due to poor resol (%)	% total error due to poor resol
a	41	3.726	0.912	2.609	2.306	1.163	19.871
b	73	4.742	0.865	3.205	2.671	1.667	27.041
c	22	3.192	0.896	2.890	2.531	1.333	21.277
p	18	4.992	0.901	2.810	2.500	1.248	19.727
q	38	3.685	0.926	2.422	2.224	0.924	14.552
s	17	2.767	0.874	3.108	2.648	1.555	25.049
For the above run: $\sigma_m = 9.2\%$							
$\theta^2 = 25,000 \text{ sec}^2$		residual variance = 213.6642 sec ²		variance improvement = 68.75%			
a	41	3.366	0.855	2.418	2.022	1.278	27.958
b	73	4.082	0.793	2.885	2.243	1.738	36.283
c	22	2.916	0.830	2.662	2.193	1.461	30.106
p	18	4.409	0.836	2.605	2.174	1.399	28.842
q	38	3.467	0.872	2.293	2.005	1.080	22.203
s	17	2.445	0.802	2.822	2.246	1.650	34.165
For the above run: $\sigma_m = 6.6\%$							
$\theta^2 = 50,000 \text{ sec}^2$		residual variance = 218.6743 sec ²		variance improvement = 68.02%			
a	41	3.149	0.812	2.291	1.842	1.320	33.209
b	73	3.672	0.742	2.685	1.989	1.740	42.014
c	22	2.728	0.781	2.511	1.978	1.505	35.921
p	18	4.052	0.787	2.465	1.967	1.451	34.658
q	38	3.295	0.829	2.200	1.854	1.156	27.597
s	17	2.270	0.750	2.639	2.004	1.667	39.871
For the above run: $\sigma_m = 5.4\%$							
$\theta^2 = 75,000 \text{ sec}^2$		residual variance = 223.5098 sec ²		variance improvement = 67.31%			
a	41	2.989	0.777	2.196	1.712	1.338	37.121
b	73	3.381	0.701	2.540	1.813	1.725	46.116
c	22	2.585	0.740	2.397	1.823	1.521	40.262
p	18	3.794	0.747	2.358	1.817	1.471	38.902
q	38	3.153	0.793	2.127	1.739	1.199	31.781
s	17	2.145	0.709	2.506	1.834	1.662	44.019
For the above run: $\sigma_m = 4.8\%$							
$\theta^2 = 100,000 \text{ sec}^2$		residual variance = 228.1161 sec ²		variance improvement = 66.64%			
a	41	2.748	0.720	2.059	1.529	1.348	42.846
b	73	2.982	0.639	2.337	1.576	1.682	51.842
c	22	2.374	0.677	2.232	1.604	1.523	46.572
p	18	3.419	0.683	2.202	1.608	1.477	44.981
q	38	2.926	0.733	2.015	1.568	1.243	38.076
s	17	1.959	0.646	2.315	1.601	1.636	49.928
For the above run: $\sigma_m = 4.0\%$							
$\theta^2 = 150,000 \text{ sec}^2$		residual variance = 236.7157 sec ²		variance improvement = 65.38%			

Table 6

Period 30 sec. For this period: initial data variance = 418.0665 sec²; No. of observations = 1669; No. blocks = 448; average path length = 6176.123 km.

Region	Number of blocks studied	RMS vel variations (%)	Average resolution	Aver total STD dev (%)	Aver STD dev due to Random error (%)	Aver STD dev due to poor resol (%)	% total error due to poor resol
a	54	2.839	0.926	1.982	1.738	0.869	19.251
b	137	3.420	0.864	2.689	2.141	1.505	31.316
c	62	2.977	0.834	2.898	2.162	1.764	37.082
p	51	2.991	0.825	2.927	2.067	1.890	41.663
q	110	3.800	0.860	2.583	1.981	1.494	33.454
s	34	2.223	0.873	2.505	2.007	1.367	29.789
For the above run: $\sigma_m = 7.9\%$							
$\theta^2 = 25,000 \text{ sec}^2$ residual variance = 158.0148 sec ² variance improvement = 62.20%							
a	54	2.497	0.882	1.841	1.549	0.934	25.732
b	137	2.811	0.801	2.386	1.791	1.486	38.803
c	62	2.566	0.771	2.520	1.781	1.667	43.759
p	51	2.327	0.767	2.510	1.717	1.692	45.427
q	110	3.322	0.805	2.274	1.674	1.413	38.623
s	34	1.910	0.816	2.234	1.707	1.333	35.576
For the above run: $\sigma_m = 5.7\%$							
$\theta^2 = 50,000 \text{ sec}^2$ residual variance = 161.9616 sec ² variance improvement = 61.26%							
a	54	2.288	0.846	1.750	1.428	0.916	30.159
b	137	2.469	0.756	2.206	1.592	1.452	43.363
c	62	2.341	0.727	2.306	1.571	1.594	47.797
p	51	2.035	0.726	2.288	1.530	1.587	48.100
q	110	2.057	0.764	2.101	1.503	1.361	41.997
s	34	1.754	0.774	2.077	1.536	1.304	39.416
For the above run: $\sigma_m = 4.7\%$							
$\theta^2 = 75,000 \text{ sec}^2$ residual variance = 165.1805 sec ² variance improvement = 60.49%							
a	54	2.135	0.817	1.681	1.338	0.974	33.571
b	137	2.238	0.720	2.078	1.455	1.419	46.650
c	62	2.186	0.693	2.159	1.429	1.537	50.689
p	51	1.855	0.693	2.140	1.405	1.517	50.245
q	110	2.870	0.732	1.981	1.386	1.323	44.573
s	34	1.648	0.740	1.966	1.417	1.280	42.370
For the above run: $\sigma_m = 4.1\%$							
$\theta^2 = 100,000 \text{ sec}^2$ residual variance = 168.0143 sec ² variance improvement = 59.81%							
a	54	1.916	0.768	1.580	1.208	0.983	38.711
b	137	1.935	0.664	1.901	1.271	1.362	51.330
c	62	1.973	0.640	1.959	1.243	1.450	54.791
p	51	1.628	0.641	1.944	1.235	1.423	53.625
q	110	2.605	0.681	1.818	1.227	1.266	48.479
s	34	1.503	0.687	1.812	1.254	1.240	46.844
For the above run: $\sigma_m = 3.4\%$							
$\theta^2 = 150,000 \text{ sec}^2$ residual variance = 172.9529 sec ² variance improvement = 58.63%							

Table 7

Period 40 sec. For this period: initial data variance = 399.0022 sec²; No. of observations = 1865; No. blocks = 479; average path length = 6426.467 km.

Region	Number of blocks studied	RMS vel variations (%)	Average resolution	Aver total STD dev (%)	Aver STD dev due to Random error (%)	Aver STD dev due to poor resol (%)	% total error due to poor resol
a	56	2.569	0.883	1.978	1.655	1.011	26.160
b	151	2.780	0.793	2.618	1.906	1.681	41.225
c	65	3.024	0.792	2.581	1.846	1.665	41.610
p	53	2.407	0.794	2.563	1.821	1.660	41.925
q	121	2.823	0.798	2.478	1.778	1.571	40.190
s	33	2.406	0.835	2.296	1.794	1.316	32.881

For the above run: $\sigma_m = 6.2\%$
 $\theta^2 = 50,000 \text{ sec}^2$ residual variance = 190.5725 sec² variance improvement = 52.24%

a	56	2.174	0.820	1.798	1.428	1.044	33.692
b	151	2.283	0.715	2.256	1.543	1.567	48.249
c	65	2.403	0.719	2.221	1.505	1.539	48.028
p	53	1.835	0.722	2.206	1.506	1.511	46.926
q	121	2.336	0.728	2.140	1.467	1.445	45.572
s	33	2.046	0.763	2.035	1.509	1.278	39.470

For the above run: $\sigma_m = 4.4\%$
 $\theta^2 = 100,000 \text{ sec}^2$ residual variance = 196.6412 sec² variance improvement = 50.72%

a	56	1.946	0.772	1.685	1.287	1.048	38.666
b	151	2.013	0.662	2.051	1.346	1.486	52.473
c	65	2.068	0.668	2.020	1.318	1.457	52.031
p	53	1.559	0.671	2.011	1.332	1.428	50.458
q	121	2.095	0.679	1.954	1.296	1.370	49.173
s	33	1.836	0.711	1.882	1.343	1.248	44.000

For the above run: $\sigma_m = 3.7\%$
 $\theta^2 = 150,000 \text{ sec}^2$ residual variance = 201.3351 sec² variance improvement = 49.54%

a	56	1.790	0.734	1.602	1.186	1.043	42.401
b	151	1.828	0.621	1.911	1.214	1.424	55.514
c	65	1.848	0.629	1.883	1.193	1.396	54.948
p	53	1.386	0.630	1.878	1.212	1.371	53.237
q	121	1.935	0.641	1.827	1.179	1.317	51.941
s	33	1.684	0.670	1.773	1.227	1.222	47.479

For the above run: $\sigma_m = 3.2\%$
 $\theta^2 = 200,000 \text{ sec}^2$ residual variance = 205.3084 sec² variance improvement = 48.55%

a	56	1.579	0.674	1.481	1.043	1.025	47.871
b	151	1.580	0.560	1.722	1.040	1.332	59.851
c	65	1.569	0.570	1.698	1.026	1.306	59.145
p	53	1.169	0.569	1.700	1.049	1.289	57.496
q	121	1.722	0.582	1.656	1.022	1.240	56.124
s	33	1.467	0.607	1.622	1.066	1.177	52.672

For the above run: $\sigma_m = 2.6\%$
 $\theta^2 = 300,000 \text{ sec}^2$ residual variance = 211.9552 sec² variance improvement = 46.88%

Table 8

Period 50 sec. For this period: initial data variance = 419.6517 sec²; No. of observations = 1867; No. blocks = 482; average path length = 6540.800 km.

Region	Number of blocks studied	RMS vel variations (%)	Average resolution	Aver total STD dev (%)	Aver STD dev due to Random error (%)	Aver STD dev due to poor resol (%)	% total error due to poor resol
a	56	2.761	0.883	2.065	1.725	1.058	26.268
b	151	2.713	0.792	2.745	1.991	1.772	41.673
c	65	3.116	0.792	2.700	1.928	1.746	41.856
p	54	2.717	0.787	2.716	1.916	1.774	42.659
q	122	2.734	0.793	2.613	1.853	1.671	40.917
s	34	3.055	0.826	2.467	1.916	1.435	33.809

For the above run: $\sigma_m = 6.4\%$

$\theta^2 = 50,000 \text{ sec}^2$ residual variance = 208.3203 sec² variance improvement = 50.36%

a	56	2.295	0.820	1.876	1.488	1.089	33.688
b	151	2.223	0.714	2.361	1.608	1.645	48.588
c	65	2.495	0.719	2.320	1.571	1.610	48.173
p	54	2.228	0.714	2.330	1.576	1.608	47.632
q	122	2.266	0.724	2.250	1.526	1.527	46.098
s	34	2.454	0.751	2.178	1.600	1.388	40.588

For the above run: $\sigma_m = 4.6\%$

$\theta^2 = 100,000 \text{ sec}^2$ residual variance = 214.7183 sec² variance improvement = 48.83%

a	56	2.037	0.773	1.757	1.342	1.092	38.623
b	151	1.962	0.661	2.145	1.402	1.558	52.744
c	65	2.157	0.669	2.110	1.376	1.523	52.122
p	54	1.961	0.663	2.120	1.390	1.516	51.104
q	122	2.023	0.675	2.051	1.347	1.445	49.624
s	34	2.145	0.698	2.009	1.417	1.351	45.191

For the above run: $\sigma_m = 3.8\%$

$\theta^2 = 150,000 \text{ sec}^2$ residual variance = 219.7206 sec² variance improvement = 47.64%

a	56	1.861	0.735	1.670	1.237	1.086	42.339
b	151	1.786	0.621	1.997	1.264	1.491	55.739
c	65	1.932	0.630	1.966	1.245	1.458	55.010
p	54	1.779	0.623	1.978	1.262	1.451	53.833
q	122	1.860	0.637	1.916	1.225	1.387	52.356
s	34	1.938	0.656	1.890	1.290	1.319	48.695

For the above run: $\sigma_m = 3.3\%$

$\theta^2 = 200,000 \text{ sec}^2$ residual variance = 223.9850 sec² variance improvement = 46.63%

a	56	1.626	0.675	1.544	1.088	1.067	47.788
b	151	1.549	0.560	1.798	1.012	1.393	60.019
c	65	1.635	0.570	1.773	1.071	1.364	59.177
p	54	1.532	0.562	1.787	1.090	1.361	58.020
q	122	1.643	0.579	1.735	1.061	1.304	56.501
s	34	1.661	0.592	1.723	1.115	1.265	53.881

For the above run: $\sigma_m = 2.8\%$

$\theta^2 = 300,000 \text{ sec}^2$ residual variance = 231.1445 sec² variance improvement = 44.92%

Table 9

Period 60 sec. For this period: initial data variance = 421.5191 sec²; No. of observations = 1779; No. blocks = 456; average path length = 6662.692 km.

Region	Number of blocks studied	RMS vel variations (%)	Average resolution	Aver total STD dev (%)	Aver STD dev due to Random error (%)	Aver STD dev due to poor resol (%)	% total error due to poor resol
a	55	2.066	0.770	1.819	1.380	1.142	39.380
b	147	2.139	0.672	2.180	1.458	1.563	51.443
c	60	1.890	0.709	2.058	1.438	1.425	47.971
p	50	1.684	0.710	2.053	1.486	1.372	44.634
q	111	1.970	0.724	1.977	1.434	1.304	43.528
s	33	2.007	0.730	1.982	1.498	1.261	40.459

For the above run: $\sigma_m = 3.9\%$

$\theta^2 = 150,000 \text{ sec}^2$ residual variance = 231.6534 sec² variance improvement = 45.04%

a	55	1.877	0.732	1.726	1.269	1.133	43.076
b	147	1.926	0.630	2.033	1.315	1.502	54.629
c	60	1.713	0.668	1.929	1.305	1.381	51.225
p	50	1.501	0.666	1.934	1.353	1.343	48.242
q	111	1.814	0.683	1.864	1.309	1.278	46.991
s	33	1.827	0.686	1.877	1.365	1.255	44.699

For the above run: $\sigma_m = 3.4\%$

$\theta^2 = 200,000 \text{ sec}^2$ residual variance = 235.9013 sec² variance improvement = 44.03%

a	55	1.735	0.700	1.653	1.184	1.121	46.021
b	147	1.768	0.596	1.922	1.209	1.452	57.115
c	60	1.581	0.635	1.831	1.206	1.342	53.767
p	50	1.371	0.630	1.841	1.252	1.317	51.130
q	111	1.697	0.649	1.776	1.213	1.253	49.753
s	33	1.698	0.649	1.794	1.264	1.243	48.034

For the above run: $\sigma_m = 3.1\%$

$\theta^2 = 250,000 \text{ sec}^2$ residual variance = 239.6021 sec² variance improvement = 43.16%

a	55	1.623	0.672	1.592	1.114	1.108	48.463
b	147	1.645	0.568	1.832	1.126	1.409	59.154
c	60	1.477	0.607	1.751	1.128	1.309	55.854
p	50	1.271	0.600	1.765	1.171	1.292	53.538
q	111	1.604	0.620	1.705	1.137	1.230	52.052
s	33	1.600	0.618	1.725	1.182	1.229	50.775

For the above run: $\sigma_m = 2.8\%$

$\theta^2 = 300,000 \text{ sec}^2$ residual variance = 242.8998 sec² variance improvement = 42.37%

a	55	1.533	0.648	1.541	1.056	1.095	50.545
b	147	1.544	0.543	1.759	1.058	1.372	60.880
c	60	1.392	0.582	1.685	1.063	1.279	57.626
p	50	1.192	0.573	1.702	1.103	1.269	55.598
q	111	1.528	0.595	1.645	1.073	1.209	54.022
s	33	1.520	0.591	1.666	1.113	1.214	53.093

For the above run: $\sigma_m = 2.6\%$

$\theta^2 = 350,000 \text{ sec}^2$ residual variance = 245.8863 sec² variance improvement = 41.67%

Table 10

Period 70 sec. For this period: initial data variance = 448.7001 sec²; No. of observations = 1650; No. blocks = 445; average path length = 6756.104 km.

Region	Number of blocks studied	RMS vel variations (%)	Average resolution	Aver total STD dev (%)	Aver STD dev due to Random error (%)	Aver STD dev due to poor resol (%)	% total error due to poor resol
a	55	1.971	0.717	1.752	1.268	1.171	44.692
b	141	1.912	0.619	2.039	1.300	1.524	55.849
c	59	1.676	0.662	1.929	1.302	1.389	51.881
p	49	1.615	0.653	1.952	1.342	1.380	49.979
q	108	1.839	0.677	1.864	1.300	1.290	47.885
s	33	1.880	0.672	1.897	1.353	1.297	46.750

For the above run: $\sigma_m = 3.4\%$

$\theta^2 = 200,000 \text{ sec}^2$ residual variance = 229.8752 sec² variance improvement = 48.77%

a	55	1.827	0.684	1.676	1.180	1.157	47.630
b	141	1.747	0.585	1.927	1.195	1.471	58.261
c	59	1.534	0.628	1.831	1.203	1.351	54.460
p	49	1.496	0.616	1.857	1.241	1.350	52.803
q	108	1.716	0.642	1.777	1.205	1.264	50.635
s	33	1.775	0.635	1.810	1.251	1.280	49.959

For the above run: $\sigma_m = 3.0\%$

$\theta^2 = 250,000 \text{ sec}^2$ residual variance = 233.9635 sec² variance improvement = 47.86%

a	55	1.712	0.656	1.614	1.110	1.142	50.058
b	141	1.618	0.557	1.837	1.113	1.426	60.246
c	59	1.424	0.599	1.753	1.124	1.318	56.569
p	49	1.401	0.586	1.780	1.159	1.322	55.156
q	108	1.618	0.613	1.706	1.130	1.241	52.920
s	33	1.690	0.604	1.739	1.169	1.262	52.598

For the above run: $\sigma_m = 2.8\%$

$\theta^2 = 300,000 \text{ sec}^2$ residual variance = 237.6208 sec² variance improvement = 47.04%

a	55	1.617	0.632	1.561	1.051	1.137	52.122
b	141	1.514	0.532	1.764	1.046	1.388	61.931
c	59	1.336	0.574	1.687	1.059	1.289	58.352
p	49	1.323	0.559	1.715	1.092	1.297	57.169
q	108	1.537	0.588	1.646	1.067	1.219	54.874
s	33	1.620	0.577	1.679	1.101	1.243	54.833

For the above run: $\sigma_m = 2.6\%$

$\theta^2 = 350,000 \text{ sec}^2$ residual variance = 240.9366 sec² variance improvement = 46.30%

a	55	1.537	0.610	1.515	1.001	1.112	53.914
b	141	1.427	0.511	1.701	0.989	1.354	63.392
c	59	1.263	0.552	1.631	1.005	1.262	59.897
p	49	1.258	0.536	1.659	1.034	1.274	58.924
q	108	1.468	0.566	1.594	1.013	1.199	56.579
s	33	1.559	0.554	1.627	1.044	1.226	56.766

For the above run: $\sigma_m = 2.5\%$

$\theta^2 = 400,000 \text{ sec}^2$ residual variance = 243.9740 sec² variance improvement = 45.63%

Table 11

Period 80 sec. For this period: initial data variance = 493.0962 sec²; No. of observations = 1533; No. blocks = 442; average path length = 6884.480 km.

Region	Number of blocks studied	RMS vel variations (%)	Average resolution	Aver total STD dev (%)	Aver STD dev due to Random error (%)	Aver STD dev due to poor resol (%)	% total error due to poor resol
a	54	2.080	0.706	1.874	1.340	1.273	46.145
b	140	1.879	0.607	2.171	1.364	1.642	57.232
c	59	1.594	0.652	2.049	1.371	1.489	52.804
p	49	1.646	0.640	2.080	1.409	1.493	51.494
q	107	1.900	0.664	1.990	1.371	1.397	49.283
s	33	1.831	0.654	2.040	1.419	1.432	49.267
For the above run: $\sigma_m = 3.5\%$							
$\theta^2 = 200,000 \text{ sec}^2$ residual variance = 251.1567 sec ² variance improvement = 49.06%							
a	54	1.936	0.672	1.790	1.244	1.254	49.104
b	140	1.721	0.573	2.048	1.252	1.581	59.588
c	59	1.479	0.618	1.943	1.265	1.446	55.379
p	49	1.532	0.604	1.975	1.300	1.455	54.278
q	107	1.768	0.630	1.894	1.268	1.366	52.021
s	33	1.720	0.617	1.941	1.308	1.405	52.362
For the above run: $\sigma_m = 3.2\%$							
$\theta^2 = 250,000 \text{ sec}^2$ residual variance = 255.5379 sec ² variance improvement = 48.18%							
a	54	1.819	0.644	1.721	1.168	1.235	51.534
b	140	1.599	0.544	1.951	1.165	1.530	61.525
c	59	1.389	0.589	1.858	1.180	1.409	57.483
p	49	1.441	0.573	1.891	1.212	1.422	56.591
q	107	1.664	0.600	1.816	1.187	1.338	54.290
s	33	1.628	0.586	1.861	1.220	1.379	54.895
For the above run: $\sigma_m = 2.9\%$							
$\theta^2 = 300,000 \text{ sec}^2$ residual variance = 259.4882 sec ² variance improvement = 47.37%							
a	54	1.720	0.619	1.663	1.104	1.217	53.591
b	140	1.500	0.520	1.871	1.093	1.487	63.170
c	59	1.316	0.563	1.787	1.112	1.376	59.262
p	49	1.366	0.546	1.820	1.140	1.393	58.565
q	107	1.579	0.575	1.751	1.119	1.313	56.225
s	33	1.550	0.559	1.794	1.147	1.355	57.034
For the above run: $\sigma_m = 2.7\%$							
$\theta^2 = 350,000 \text{ sec}^2$ residual variance = 263.0964 sec ² variance improvement = 46.64%							
a	54	1.634	0.597	1.612	1.050	1.200	55.369
b	140	1.419	0.498	1.803	1.034	1.449	64.596
c	59	1.254	0.541	1.727	1.054	1.347	60.801
p	49	1.303	0.523	1.759	1.079	1.366	60.283
q	107	1.507	0.552	1.694	1.062	1.289	57.910
s	33	1.483	0.535	1.736	1.085	1.332	58.879
For the above run: $\sigma_m = 2.6\%$							
$\theta^2 = 400,000 \text{ sec}^2$ residual variance = 266.4241 sec ² variance improvement = 45.97%							

Table 12

Period 90 sec. For this period: initial data variance = 551.8558 sec²; No. of observations = 1276; No. blocks = 424; average path length = 7220.475 km.

Region	Number of blocks studied	RMS vel variations (%)	Average resolution	Aver total STD dev (%)	Aver STD dev due to Random error (%)	Aver STD dev due to poor resol (%)	% total error due to poor resol
a	53	2.002	0.653	1.784	1.216	1.278	51.305
b	131	1.579	0.560	2.015	1.219	1.570	60.747
c	58	1.471	0.590	1.948	1.224	1.490	58.480
p	46	1.795	0.570	1.997	1.258	1.525	58.296
q	103	1.663	0.603	1.904	1.242	1.408	54.716
s	33	1.618	0.552	2.039	1.266	1.574	59.609
For the above run: $\sigma_m = 3.1\%$							
$\theta^2 = 250,000 \text{ sec}^2$ residual variance = 238.4564 sec ² variance improvement = 56.79%							
a	53	1.880	0.624	1.716	1.140	1.258	53.730
b	131	1.466	0.531	1.921	1.134	1.521	62.689
c	58	1.393	0.561	1.862	1.142	1.448	60.447
p	46	1.682	0.539	1.909	1.171	1.485	60.483
q	103	1.560	0.573	1.825	1.160	1.378	56.961
s	33	1.494	0.521	1.947	1.173	1.532	61.900
For the above run: $\sigma_m = 2.8\%$							
$\theta^2 = 300,000 \text{ sec}^2$ residual variance = 243.2100 sec ² variance improvement = 55.93%							
a	53	1.780	0.599	1.659	1.077	1.239	55.769
b	131	1.376	0.506	1.844	1.064	1.479	64.332
c	58	1.330	0.536	1.791	1.075	1.411	62.107
p	46	1.590	0.513	1.836	1.099	1.449	62.334
q	103	1.477	0.547	1.760	1.093	1.350	58.867
s	33	1.394	0.495	1.870	1.098	1.494	63.810
For the above run: $\sigma_m = 2.6\%$							
$\theta^2 = 350,000 \text{ sec}^2$ residual variance = 247.4798 sec ² variance improvement = 55.15%							
a	53	1.695	0.577	1.609	1.024	1.220	57.523
b	131	1.302	0.484	1.779	1.006	1.442	65.754
c	58	1.276	0.514	1.730	1.018	1.379	63.544
p	46	1.515	0.490	1.773	1.039	1.418	63.935
q	103	1.409	0.524	1.703	1.036	1.325	60.522
s	33	1.310	0.472	1.805	1.035	1.460	65.441
For the above run: $\sigma_m = 2.5\%$							
$\theta^2 = 400,000 \text{ sec}^2$ residual variance = 251.3674 sec ² variance improvement = 54.45%							
a	53	1.557	0.539	1.525	0.937	1.186	60.422
b	131	1.185	0.448	1.672	0.913	1.380	68.119
c	58	1.189	0.477	1.630	0.927	1.324	65.941
p	46	1.395	0.452	1.670	0.942	1.363	66.595
q	103	1.300	0.486	1.609	0.944	1.280	63.285
s	33	1.180	0.434	1.697	0.934	1.400	68.113
For the above run: $\sigma_m = 2.3\%$							
$\theta^2 = 500,000 \text{ sec}^2$ residual variance = 258.2618 sec ² variance improvement = 53.20%							

Table 13

Period 98 sec. For this period: initial data variance = 536.8802 sec²; No. of observations = 954; No. blocks = 391; average path length = 7734.103 km.

Region	Number of blocks studied	RMS vel variations (%)	Average resolution	Aver total STD dev (%)	Aver STD dev due to Random error (%)	Aver STD dev due to poor resol (%)	% total error due to poor resol
a	52	1.571	0.584	1.711	1.088	1.302	57.925
b	115	1.312	0.507	1.865	1.076	1.501	64.758
c	55	1.173	0.529	1.823	1.073	1.453	63.556
p	41	1.606	0.498	1.886	1.095	1.517	64.739
q	97	1.617	0.529	1.816	1.103	1.418	60.934
s	31	1.420	0.446	1.982	1.077	1.647	69.059

For the above run: $\sigma_m = 2.7\%$
 $\theta^2 = 300,000 \text{ sec}^2$ residual variance = 216.0930 sec² variance improvement = 59.75%

a	52	1.483	0.558	1.653	1.026	1.280	59.887
b	115	1.231	0.482	1.793	1.011	1.460	66.355
c	55	1.115	0.504	1.754	1.011	1.415	65.089
p	41	1.523	0.472	1.813	1.028	1.477	66.388
q	97	1.535	0.503	1.751	1.038	1.387	62.755
s	31	1.323	0.421	1.899	1.006	1.596	70.641

For the above run: $\sigma_m = 2.5\%$
 $\theta^2 = 350,000 \text{ sec}^2$ residual variance = 221.2085 sec² variance improvement = 58.80%

a	52	1.410	0.535	1.604	0.974	1.258	61.564
b	115	1.164	0.460	1.732	0.957	1.425	67.736
c	55	1.066	0.483	1.696	0.959	1.382	66.422
p	41	1.453	0.450	1.751	0.972	1.442	67.822
q	97	1.466	0.480	1.695	0.984	1.359	64.334
s	31	1.244	0.400	1.830	0.946	1.552	71.993

For the above run: $\sigma_m = 2.4\%$
 $\theta^2 = 400,000 \text{ sec}^2$ residual variance = 225.8989 sec² variance improvement = 57.92%

a	52	1.349	0.515	1.560	0.930	1.239	63.025
b	115	1.107	0.441	1.679	0.910	1.394	68.952
c	55	1.024	0.463	1.645	0.914	1.353	67.600
p	41	1.393	0.430	1.698	0.924	1.411	69.087
q	97	1.405	0.460	1.646	0.936	1.334	65.724
s	31	1.177	0.381	1.769	0.895	1.514	73.170

For the above run: $\sigma_m = 2.3\%$
 $\theta^2 = 450,000 \text{ sec}^2$ residual variance = 230.2374 sec² variance improvement = 57.11%

a	52	1.296	0.498	1.522	0.891	1.220	64.316
b	115	1.057	0.423	1.632	0.869	1.366	70.035
c	55	0.987	0.446	1.601	0.875	1.326	68.654
p	41	1.341	0.412	1.651	0.881	1.383	70.218
q	97	1.351	0.442	1.603	0.895	1.312	66.963
s	31	1.119	0.365	1.717	0.852	1.479	74.211

For the above run: $\sigma_m = 2.2\%$
 $\theta^2 = 500,000 \text{ sec}^2$ residual variance = 234.2789 sec² variance improvement = 56.36%

diagonal element of the resolution matrix, calculated using eq. (10); the standard deviation due to random noise, given by eq. (11); and the standard error due to poor resolution.

In Tab. 5 through 13 we show the above parameters averaged for each region symbol of the initial model of Jordan (1981), for a number of inversions using different damping constants. At the top of each of these tables, we indicated the period studied; the initial data variance, the number of observations used, the number of blocks resolved, and the average path length, all for the period in question. For each run, we showed the residual variance, and the variance improvement. Also shown is the square root of the model variance σ_m^2 corresponding to the choice of damping constant.

The damping constant selected for the final solution for each of the reference periods are underlined in each of these tables. The selection was made considering the trade-off between errors and resolution of each solution, so that an acceptable balance was achieved. The values of σ_m are, in many cases, comparable to those obtained for the standard deviation of the regionalized Earth models (tabulated by Rosa & Aki, 1991).

An interesting comparison can be made between the standard deviation of our phase travel time residual data with that used by Yomogida (1985), which is shown in Tab. 14a. We can see that the two sets are very similar, although Yomogida (1985) studied paths restricted to the Pacific basin. A more interesting comparison in Tab. 14b is between the residual standard deviation of the inversion results of our work and that of Forsyth (1975), by regionalization with four oceanic, and two continental regions including the anisotropy. In the same table, we also show the result of Patton (1978), who used a regionalized model consisting of five regions to fit his observations of phase velocity for Rayleigh waves propagating in Eurasia. Also shown in Tab. 14b is the residual standard deviation reported by Patton (1984), for phase velocity data of Rayleigh waves in the Western U.S.. Patton (1984) used four major provinces, and three 'less distinct' provinces, to explain up to 40 percent of the initial variance of phase velocity data of Rayleigh waves with 40 sec period. Finally, we showed the residual standard deviation obtained by Yomogida (1985) by the inversion of phase data only.

From these data shown in Tab. 14b, we notice that the residual standard deviation achieved in our work is larger than that obtained by Forsyth (1975) and by Patton (1984), who studied much smaller regions. Our residual standard deviation is comparable to the result of Yomogida (1985) for the Pacific region, where he used a 5° by 5° regionalization grid.

The resulting phase velocity world maps (consisting of the initial velocity model plus perturbation) obtained by each computer run corresponding to a chosen damping constant are

Table 14a. Standard deviation of the travel time residual data (sec).

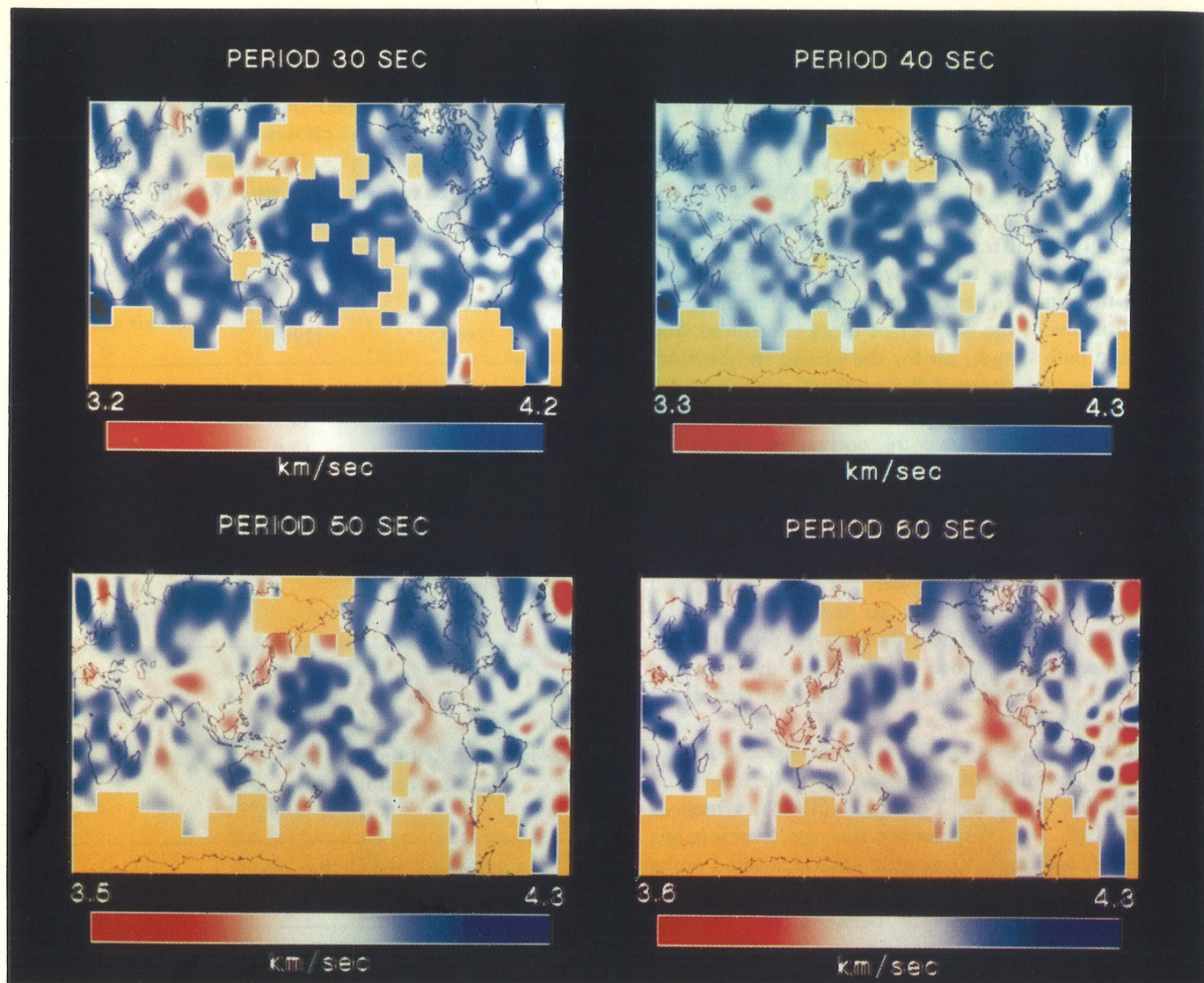
Period (sec)	Yomogida (1985)	This work
20	-	23.15
30	18.7	20.45
40	17.0	19.97
50	-	20.48
60	16.5	20.53
70	-	21.18
80	14.9	22.20
90	-	23.49
98	-	23.17

Table 14b. Residual standard deviation after inversion (sec).

Period (sec)	Forsyth (1975)	Patton (1978)
26	6.5	15.8
34	5.5	11.9
40	4.8	9.7
66	5.1	8.0
90	6.2	8.3

Period (sec)	Patton (1984)	Yomogida (1985)	This work
20		-	14.79 (68.02%)
30		13.8 (45.5%)	12.85 (60.49%)
40		12.3 (47.6%)	14.02 (50.72%)
50	4-6 (40%)	-	14.82 (47.64%)
60		13.1 (36.5%)	15.36 (44.03%)
70		-	15.29 (47.86%)
80		12.9 (24.8%)	16.11 (47.37%)
90		-	15.73 (55.15%)
98		-	14.87 (58.80%)

In this last table we also show the variance improvement for each case.



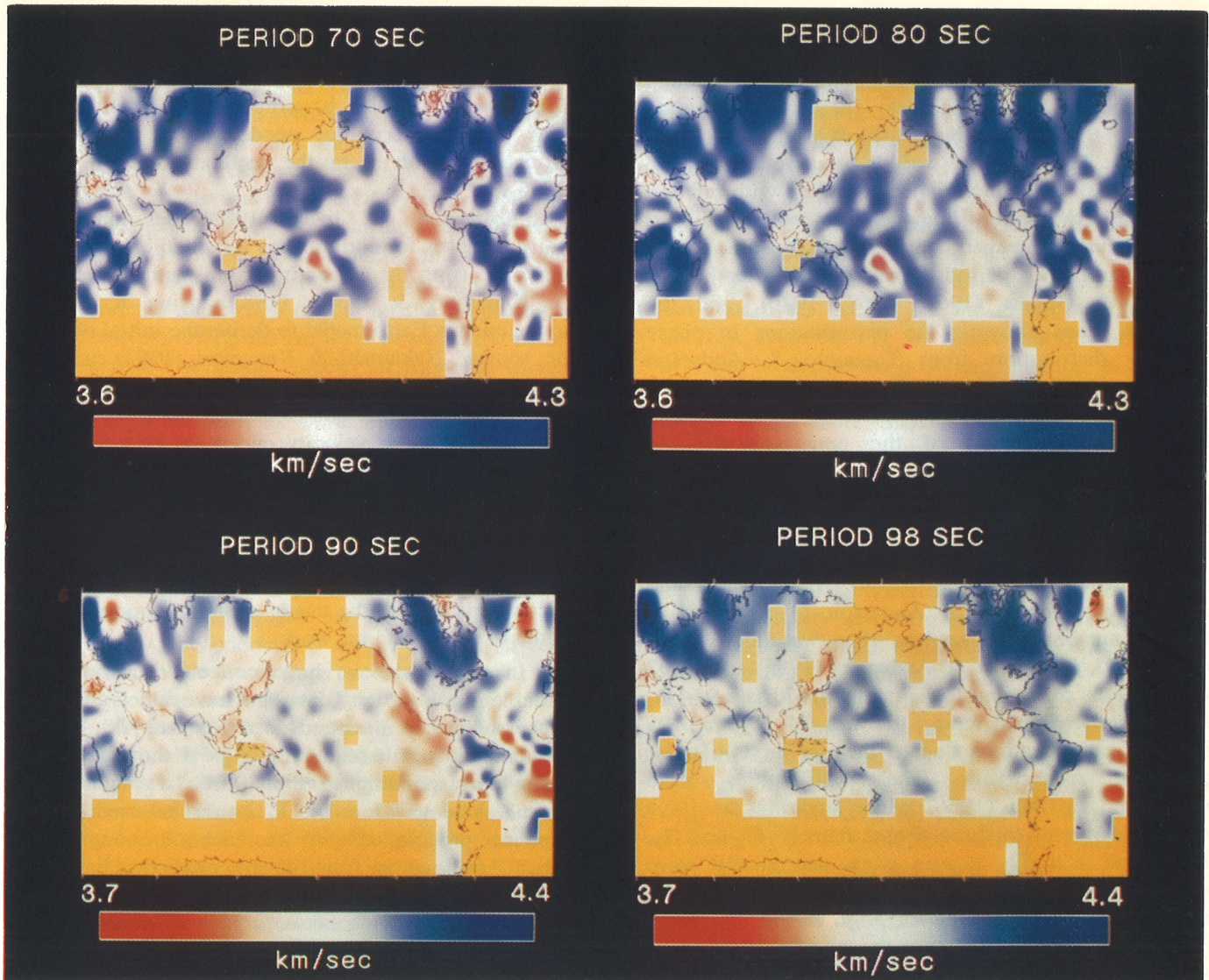
Figures 1 through 4. Resulting phase velocity global maps for the reference periods from 30 through 60 sec, respectively.

Figuras 1 a 4. Mapas de velocidade de fase obtidos, respectivamente, para os valores de período de 30 a 60 segundos.

plotted in Figs. 1 through 8, for the reference periods 30 through 98 sec. The velocity perturbation maps, the data density, the diagonal element of the resolution matrix, the total standard deviation, and the standard deviation due to random noise in the data, are all plotted in the work of Rosa (1986) and were not included here for simplicity. Each of these maps is shown in the mercator projection, with the latitude ranging from 70°S to 75°N. We have used a bi-cubic spline interpolation scheme (de Boor, 1978) to interpolate between the values corresponding to each block studied. We expected to obtain some of the abnormal effects at the borders of the maps and in areas close to unresolved blocks (shown either as yellow or in black in these figures), due to the lack of

continuity of values in such cases. So, we ignored anomalies which are too close to these borders. Other regions for which we kept some conservative view when analyzing the results are those too close to the polar regions.

In general, the diagonal elements of the resolution matrix (Rosa, 1986) approaches unity for blocks with the largest number of hits. This increasing of resolution of the solution is also associated with a decrease in total standard deviation, and a decrease in the values of standard deviation associated with random error, in a way that the most reliable part of the result is in areas where the data coverage was the best (such as in North America, the East Pacific, the North Atlantic, western Europe, East Africa, northern



Figures 5 through 8. Resulting phase velocity global maps for the reference periods from 70 through 98 sec, respectively.

Figuras 5 a 8. Mapas de velocidade de fase obtidos, respectivamente, para os valores de período de 70 a 98 segundos.

portions of the Indian Ocean, and the Tibet region).

Anomalies in phase velocity for the period range studied reflect possible differences in body wave seismic velocities and densities in the crust and upper mantle structure of the several regions considered. These differences can be caused by temperature anomalies, compositional variations, partial melting, and anisotropy. Many of these features were noticeable by previous small-scale works, or were expected by the known tectonic setting of several regions.

In the Pacific region, a comparison can be made between our results and those of Yomogida (1985) in the corresponding reference periods. In this case, both maps corresponding to phase velocity changes, and

maps of these velocity distribution show much resemblance, with most of the major anomalies represented in both results. The results of Nishimura & Forsyth (1985) on the Love wave phase velocity distribution on the Pacific basin also provided us with another opportunity to check our results in this region (Rosa, 1986).

As we mentioned earlier, there have been a number of recent works on the global distribution of phase and group velocity of Rayleigh and Love waves with period greater than the period range studied in this paper. Rosa (1986) reviewed these efforts in greater detail.

Among these longer-period global studies, Tanimoto & Anderson (1984, 1985) studied the lateral

variation of phase velocity of long period surface waves (R_2 , R_3 and G_2 , G_3) and the azimuthal dependence of these velocities. They inverted a data set larger than that of Nakanishi & Anderson (1983, 1984a, b). The reference periods used were 100, 150, 200 and 250 sec. The variance reduction with relation to an initially laterally homogeneous model achieved in their work are respectively 45.8, 64.9, 66.6, 54.5% at these reference periods. They used the method of Backus & Gilbert (1967, 1968, 1970), and the resultant maps showing the perturbations in phase velocity distribution from Tanimoto & Anderson (1985) and Tanimoto (1985) were later used by Tanimoto (1986) in the determination of the SH and SV velocity structure of the upper mantle. As described in Rosa (1986), our results at 98 sec compare well with those obtained by Tanimoto & Anderson (1985) for the reference period 100 sec. For 100 sec, their inversion achieved about 46% variance improvement, compared to 59% of ours. One could argue that Tanimoto & Anderson (1985) used a smaller number of unknowns than we did. On the other hand, Tanimoto & Anderson (1985) used 497 observations of R_2 and R_3 in contrast with our 954 R_1 observations. Furthermore, the use of R_2 and R_3 involves complications due to the one or two polar passages, respectively. These difficulties were considered by Aki (1966) while studying the Love wave equivalents to these phases namely, G_2 and G_3 . He found that G_3 phases were particularly more complicated, and we expect to find the same difficulties when analyzing Rayleigh waves.

We should also discuss the possibility of using our phase velocity maps for application of the moment tensor inversion method to study the mechanism of any earthquake in the Earth.

Weidner (1972), using the reference point method described by Weidner & Aki (1973), was able to almost completely separate the source and path effects of earthquakes in the Atlantic using event pairs. Patton (1978) achieved a similar goal, by using a group of events located around a reference point in Tibet.

An early estimate of the accuracy needed for the phase velocity values in all paths connecting stations and source point, in order to separate the propagation effect from the phase observations prior to the linear moment tensor inversion method of Mendiguren (1977), was made by Aki & Patton (1978). They estimated that, for this case, we need 0.5% accuracy in the phase velocity data. This corresponds to saying that, for a path measuring a few thousand kilometers, we have an error of a few seconds in the travel time of the observed phase.

Patton (1978) was able to achieve such accuracy

with the application of the reference point method, but not with his regionalized map of phase velocity. Romanowicz (1982a, b) proposed an alternative to relax the high accuracy needed in the propagation correction involved in the method used by Patton (1978).

Kanamori & Given (1982) determined the moment tensor for earthquakes recorded by the I.D.A. network, using the linear inversion method described by Kanamori & Given (1981) using a laterally homogeneous Earth model to derive the initial phase at the source. Nakanishi & Kanamori (1982) used the same method to study surface waves with period ranging between 197 and 256 sec, this time with the regionalized phase velocity curves of Dziewonski & Steim (1982), and a discretized world map representation with grid size $5^\circ \times 5^\circ$ similar to those used by Rosa & Aki (1991). Their conclusion was that the simple regionalized phase velocity curves have improved the linear inversion for the moment tensor, in comparison with the use of a laterally homogeneous media of their previous work.

In our work, we have collected most of the available phase velocity data, and have added a greater number of newly measured data (Rosa & Aki, 1991), to obtain the results shown in Figs. 1 through 8 (the results corresponding to the 20 sec waves are not shown, since too few blocks could be used in the inversion process, due to the lack of enough data paths). As shown in Tab. 14b, the prediction based on the phase velocity mapping with the $10^\circ \times 10^\circ$ meshes gave residuals ranging between 13 and 16 sec for all periods. Clearly, our results cannot be used in the application of the moment tensor inversion method to any event using the waves with period 20 or 30 sec, because the phase uncertainty is more than 0.5 cycles. On the other hand, if we use long period, say 100 sec, the residual is equivalent to a 0.15 cycles error which is comparable to the scatter of the phase observations in some well-constrained focal mechanism studies using Rayleigh waves (e.g. Patton, 1980). It is a very encouraging result, specially because using the moment tensor inversion at 100 sec is a great improvement when we consider that the smallest period considered by Nakanishi & Kanamori (1982) was about 200 sec. On the other hand, if we want to lower the applicability of the moment tensor inversion method from 100 sec to about 30 sec, it is necessary to improve our phase velocity maps for the shorter periods.

APPLICATION OF THE STOCHASTIC INVERSION TO THE GROUP VELOCITY DATA SET

Tetsuo A. Santo pioneered the studies on the

determination of the global distribution of the group velocity of fundamental mode Rayleigh waves (Santo, 1960a, b, 1961a, b, 1963, 1965a, b, 1966, 1967, 1968; Santo & Sato, 1966 and Sato & Santo, 1969). Regionalization of group velocity for Rayleigh waves with longer periods was considered by other workers, such as Savage & White (1969), in the Pacific Ocean, and Tarr (1969) in the North Atlantic and Caribbean Sea. Forsyth (1973) considered several types of models and the anisotropy effects on the propagation of these waves, to regionalize a set of measured paths in the Pacific. The group velocity of Rayleigh waves propagating in the Pacific was further studied by Yoshii (1975), and later by Yu & Mitchell (1979) and Mitchell & Yu (1980).

In this section, we describe an attempt to invert the group velocity collected by Rosa (1986) using the same method applied to determine the global distribution of phase velocity.

Since most of the paths used in the phase velocity study are the same as those in the group velocity study, the operator G of eq. (4) will be very similar between the two inverse problems.

We used the same regionalization (Jordan, 1981) used in the phase velocity part of this work, with group velocity values given by Rosa & Aki (1991) as our initial model. We have eliminated the rays which showed the absolute value of the residual travel time larger than four percent of the total travel time, and required that only blocks with more than 20 ray crossings be included in the inversion process. For each run, in a similar fashion to the procedure followed in the phase velocity study, we calculated the root mean square of the velocity variations, the average value of the diagonal element of the resolution

matrix, the average total standard deviation, the average standard deviation due to random error in the data, the average standard deviation due to the poor resolution, and the percentage of the total standard deviation which is represented by this latter variable.

If we consider the data at 50 sec period, we notice that the most striking difference between this data set and the phase velocity data set is the initial data variance of these two: we found that $\langle d^2 \rangle$ is about four times greater for the group velocity data (Tab. 15). From eq. (4), we notice that the difference $\langle d^2 \rangle$ can be due to the difference in either m or in n. In other words, we need to know if group velocity actually varies more than phase velocity over the Earth's surface, or if group velocity measurements have more errors than the phase velocity ones.

If we consider the first of these possibilities, we are assuming that $\sigma_{mU}^2 > \sigma_{mc}^2$, but $\sigma_{nU}^2 \equiv \sigma_{nc}^2$. In this case, the damping constant for the group velocity inversion should be chosen four times smaller than in the phase velocity inversion procedure. We tried this possibility and found solutions with unacceptable standard errors (i.e. the resulting velocity variations were insignificant comparing with their errors).

We can compare the regionalized group velocity models of Rosa & Aki (1991) with their corresponding phase velocity models, and try to verify the possibility if $\sigma_{mU}^2 > \sigma_{mc}^2$. Consider the case of 50 sec waves, for which the signal to noise ratio is larger than in other cases. We did not see any major difference between σ_{mU} and σ_{mc} in this case. So, the first possibility is unlikely.

Let us now examine the second possibility that the noise variance (measurement error) may be different between group and phase velocity data. The

Table 15

Group velocity - period 50 sec. For this period: initial data variance = 1866.2941 sec²; No. of observations = 1077; No. blocks = 225; average path length = 7788.926 km.

Region	Number of blocks studied	RMS vel variations (%)	Average resolution	Aver total STD dev (%)	Aver STD dev due to Random error (%)	Aver STD dev due to poor resol (%)	% total error due to poor resol
a	32	2.707	0.456	2.021	1.185	1.624	64.550
b	66	2.430	0.426	2.076	1.186	1.688	66.096
c	23	1.673	0.393	2.121	1.085	1.771	69.680
p	25	2.076	0.439	2.060	1.221	1.655	64.518
q	54	2.783	0.442	2.046	1.216	1.629	63.385
s	25	1.269	0.331	2.241	1.099	1.929	74.050

For the above run: σ_m 2.8%
 $\theta^2 = 1,200,000 \text{ sec}^2$ residual variance = 910.6685 sec² variance improvement = 51.20%

phase velocity is defined as the velocity at which the phase of waves (peaks, zeros and troughs) propagates, and is given by

$$c = \omega/k$$

where ω is frequency and k is wave number. The group velocity on the other hand, is the velocity of propagation of wave packet or energy with frequency ω , and is given by

$$U = d\omega/dk$$

What we are considering in the measurements of these two is the observable phase difference $\Delta\varphi(\omega)$ between two points separated by a distance Δ . The expressions for the phase and group velocities are then given by

$$1/c = (1/\Delta) (\Delta\varphi(\omega)/\omega)$$

$$1/U = (1/\Delta) [d/d\omega (\Delta\varphi(\omega))]$$

If we consider that the observed phase difference $\Delta\varphi(\omega)$ can be in error by $\Delta\varphi(\omega) \pm \delta\varphi(\omega)$, we see that the error in $1/c$ and $1/U$ are respectively,

$$\Delta[1/c] = (1/\Delta) (\delta\varphi(\omega)/\omega)$$

$$\Delta[1/U] = (1/\Delta) [\partial/\partial\omega (\delta\varphi(\omega))]$$

Thus, the error in group velocity measurement is related to the derivative of phase difference with respect to ω . If one tries to measure $1/U$ by the Fourier transform and estimating the derivative by finite difference, one can anticipate a greater error for $1/U$ than for $1/c$.

This basic difference between the accuracy of these two parameters has long been known. Evernden (1953, 1954) concluded that the phase velocity is the most important parameter to study the Earth structure using surface wave data. The same point was emphasized by Ewing & Press (1959). Other authors, such as Pilant (1967), Weidner (1972) and Soriau-Thevenard (1976), all concluded that their phase velocity measurements were much more accurate than the group velocity measurements performed for the same paths which they studied.

It is then reasonable to accept that the initial data variance of the group velocity data is much larger than the initial data variance of the phase velocity data, due to the larger measurements errors for group velocity. We accepted that this is the case and concluded that, for the group velocity inverse problem, a damping constant greater than the one used in the phase velocity study is needed in order to achieve acceptable

error levels. We list the results of one run of our inversion computer program, performed to invert the data set for waves with 50 sec period (Tab. 15). This run was performed using a constant damping constant for all blocks, as done while treating the phase velocity data. Notice that the average resolution is much lower than the level achieved in our phase velocity study. This is due to the stronger damping used here, which could not be enhanced by requiring that the blocks used had more hits than in the phase velocity study. Then, even though the result of the inversion procedure summarized in Tab. 15 showed some similarity with some major tectonic features, we do not have enough confidence in the results due to the poor resolution associated with most of the blocks studied.

As we can see in Tab. 15, the residual variance obtained in the inversion process is about four times larger than that obtained in the inversion of the corresponding phase velocity data for 50 sec waves (Tab. 8). It is also of the same order of the residual variance obtained by Feng & Teng (1983b), who inverted a similar set of group velocity data in Eurasia, using a discretized model with the same block size of our work (10^0 by 10^0). The standard deviation of their solution, listed in Tab. 4 of their work, is 29.68 sec for Rayleigh waves with period of 49.95 sec, while the standard deviation of our solution is about 30 sec for similar waves with period of 30 sec (considering the values for the residual variance listed in Tab. 15). The method used by Feng & Teng (1983b) to measure the group velocity values, discussed in a previous paper (Feng & Teng, 1983a) is of the same type of that used in our work, and show approximately the same error size. They do not show the errors and resolution associated with the solution of each one of the blocks they studied, but the similarity between our and their study indicates that the error may be greater than the variation of solution.

So, despite the widespread belief among part of the seismological community, our results show that the group velocity is much more difficult to measure and to invert than phase velocity. This is in agreement with the physical intuition about these two variables, since if we know the initial source phase, it is easier to measure the phase arrival time in an observed wave train than it is to identify the exact arrival time of a particular wave group (or energy). So, even with all the sophisticated smoothing procedures used in the group velocity measurements it is still difficult to obtain similar errors for group arrival measurements, $\delta t_U(T)$, as for those of phase arrival time measurements ($\delta t_c(T)$).

CONCLUSIONS

We have applied the stochastic inverse method to both global phase velocity and group velocity travel time data. For the phase velocity data, we found that the resulting velocity maps for longer periods can probably be used for studies of focal mechanism by the moment tensor inversion method in most of the Earth. For the lowest periods, the residual travel time obtained in the inversion suggests that we probably need a more detailed model. The original phase velocity data set for these periods can although be used as a network of reference points for focal mechanism studies.

In the case of our group velocity study, we got what is probably the most important contribution of this work: we found that since the standard deviation of the group velocity initial (regionalized) values are very similar to those in the phase velocity regionalization models (Rosa, 1986; Rosa & Aki, 1991), this shows that the large, unacceptable error bounds achieved after the application of the stochastic

inversion method to the group velocity data, are related to the larger errors involved in the measurements of the group velocity, which makes it much harder to obtain useful results from such analysis involving group velocity data. So, in spite of all the current widespread belief, this shows that the group velocity of surface waves is much more difficult to measure and to invert, just as stated by most early surface wave researchers.

ACKNOWLEDGEMENTS

This project was made possible at MIT by a NSF grant (EAR-8408714), and was supported at USC by DARPA contract F19628-85-K-0018 and by the Schlumberger-Doll Research Fund. J.W.C. Rosa's studies at MIT were supported by the Brazilian National Research Council (CNPq), process 201.022/81, while further work done for the set up of this publication was supported by CAPES, Ministry of Education, República Federativa do Brasil.

REFERENCES

- AKI, K. - 1966 - Generation and propagation of G waves from the Niigata earthquake of June 16, 1964. Part 1. A statistical analysis. *Bull. Earthq. Res. Inst.*, **44**: 23-72.
- AKI, K. - 1977 - Three dimensional seismic velocity anomalies in the lithosphere - method and summary of results. *J. Geophys.*, **43**: 235-242.
- AKI, K. - 1979 - Three-dimensional seismic anomalies and their relation to local seismicity. *Tectonophysics*, **56**: 85-88.
- AKI, K. - 1981 - 3-D inhomogeneities in the upper mantle. *Tectonophysics*, **75**: 31-40.
- AKI, K. - 1982 - Three-dimensional seismic inhomogeneities in the lithosphere and asthenosphere: evidence for decoupling in the lithosphere and flow in the asthenosphere. *Rev. Geophys. Space Phys.*, **20**: 161-170.
- AKI, K., CHRISTOFFERSSON, A. & HUSEBYE, E.S. - 1976 - Three-dimensional seismic structure of the lithosphere under Montana LASA. *Bull. Seismol. Soc. Am.*, **66**: 501-524.
- AKI, K., CHRISTOFFERSSON, A. & HUSEBYE, E.S. - 1977 - Three-dimensional seismic structure of the lithosphere. *J. Geophys. Res.*, **82**: 277-296.
- AKI, K. & LEE, W.H.K. - 1976 - Determination of three-dimensional velocity anomalies under a seismic array using first P arrival times from earthquakes. 1. A homogeneous initial model. *J. Geophys. Res.*, **81**: 4381-4399.
- AKI, K. & PATTON, H.J. - 1978 - Determination of seismic moment tensor using surface waves. *Tectonophysics*, **49**: 213-222.
- AKI, K. & RICHARDS, P.G. - 1980 - *Quantitative Seismology, Theory and Methods*. Vols. 1 and 2, W.H. Freeman, San Francisco.
- BACKUS, G.E. & GILBERT, J.F. - 1967 - Numerical applications of a formalism for geophysical inverse problems. *Geophys. J.R. astr. Soc.*, **13**: 247-276.
- BACKUS, G.E. & GILBERT, J.F. - 1968 - The resolving power of gross Earth data. *Geophys. J.R. astr. Soc.*, **16**: 169-205.
- BACKUS, G.E. & GILBERT, J.F. - 1970 - Uniqueness in the inversion of inaccurate gross Earth data. *Phil. Trans. R. Soc. Lon., A*, **266**: 123-192.
- DE BOOR, C. - 1978 - *A practical guide to splines*. Springer-Verlag, New York.
- DZIEWONSKI, A.M. & STEIM, J.M. - 1982 - Dispersion and attenuation of mantle waves through waveform inversion. *Geophys. J.R. astr. Soc.*, **70**: 503-527.
- ELLSWORTH, W.L. & KOYANAGI, R.Y. - 1977 - Three-dimensional crust and upper mantle structure beneath the Island of Hawaii. *J. Geophys. Res.*, **82**: 5379-5394.
- EVERNDEN, J.F. - 1953 - Direction of approach of Rayleigh waves and related problems. Part I. *Bull. Seismol. Soc. Am.*, **43**: 335-374.
- EVERNDEN, J.F. - 1954 - Direction of approach of Rayleigh waves and related problems. Part II. *Bull. Seismol. Soc. Am.*, **44**: 159-184.
- EWING, M. & PRESS, F. - 1959 - Determination of crustal structure from phase velocity of Rayleigh waves. Part III. The United States. *Bull. Geol. Soc. Am.*, **70**: 229-244.
- FENG, C. & TENG, T. - 1983a - An error analysis of frequency-time analysis. *Bull. Seismol. Soc. Am.*, **73**: 143-155.
- FENG, C. & TENG, T. - 1983b - Three-dimensional crust and upper mantle structure of the Eurasian Continent. *J. Geophys. Res.*, **88**: 2261-2272.

- FORSYTH, D.W. - 1973 - Anisotropy and the structural evolution of the oceanic upper mantle. PhD Thesis, Mass. Inst. of Technol., Cambridge, 253 pp.
- FORSYTH, D.W. - 1975 - The early structural evolution and anisotropy of the oceanic upper mantle. *Geophys. J.R. astr. Soc.*, **43**: 103-162.
- FRANKLIN, J.N. - 1970 - Well-posed stochastic extension of ill-posed linear problems. *J. Math. Anal. Appl.*, **31**: 682-716.
- HASEMI, A.H., ISHII, H. & TAKAGI, A. - 1984 - Fine structure beneath the Tohoku district, northeastern Japan arc, as derived by an inversion of P-wave arrival times from local earthquakes. *Tectonophysics*, **101**: 245-265.
- HIRAHARA, K. - 1977 - A large-scale three-dimensional seismic structure under the Japan Islands and the Sea of Japan. *J. Phys. Earth*, **25**: 393-417.
- HIRAHARA, K. - 1981 - Three-dimensional seismic structure beneath southwest Japan: the subducting Philippine Sea plate. *Tectonophysics*, **79**: 1-44.
- HORIE, A. & AKI, K. - 1982 - Three-dimensional velocity structure beneath the Kanto district, Japan. *J. Phys. Earth*, **30**: 255-281.
- HUSEBYE, E.S., CHRISTOFFERSSON, A., AKI, K. & POWELL, C. - 1976 - Preliminary results on the three-dimensional seismic structure of the lithosphere under the U.S.G.S. central California seismic array. *Geophys. J.R. astr. Soc.*, **46**: 319-340.
- JACKSON, D.D. - 1979 - The use of a priori data to resolve non-uniqueness in linear inversion. *Geophys. J.R. astr. Soc.*, **57**: 137-157.
- JORDAN, T.H. - 1972 - Estimation of the radial variation of seismic velocities and density of the Earth. PhD Thesis, Calif. Inst. of Technol., Pasadena.
- JORDAN, T.H. - 1981 - Global tectonic regionalization for seismological data analysis. *Bull. Seismol. Soc. Am.*, **71**: 1131-1141.
- KANAMORI, H. & GIVEN, J.W. - 1981 - Use of long-period surface waves for rapid determination of earthquake-source parameters. *Phys. Earth Planet. Inter.*, **27**: 8-31.
- KANAMORI, H. & GIVEN, J.W. - 1982 - Use of long-period surface waves for fast determination of earthquake source parameters. 2. Preliminary determination of source mechanism of large earthquake ($M_s > 6.5$) in 1980. *Phys. Earth Planet. Inter.*, **30**: 260-268.
- MENDIGUREN, J.A. - 1977 - Inversion of surface wave data in source mechanism studies. *J. Geophys. Res.*, **82**: 889-894.
- MITCHELL, B.J., CHENG, C.C. & STAUDER, W. - 1977 - A three-dimensional velocity model of the lithosphere beneath the New Madrid seismic zone. *Bull. Seismol. Soc. Am.*, **67**: 1061-1074.
- MITCHELL, B.J. & YU, G. - 1980 - Surface wave dispersion, regionalized velocity models and anisotropy of the Pacific crust and upper mantle. *Geophys. J.R. astr. Soc.*, **63**: 497-514.
- NAKANISHI, I. & ANDERSON, D.L. - 1982 - Worldwide distribution of group velocity of mantle Rayleigh waves as determined by spherical harmonic inversion. *Bull. Seismol. Soc. Am.*, **72**: 1185-1194.
- NAKANISHI, I. & ANDERSON, D.L. - 1983 - Measurements of mantle wave velocities and inversion for lateral heterogeneity and anisotropy. 1. Analysis of great circle phase velocities. *J. Geophys. Res.*, **88**: 10267-10283.
- NAKANISHI, I. & ANDERSON, D.L. - 1984a - Measurements of mantle wave velocities and inversion for lateral heterogeneity and anisotropy. 2. Analysis by the single-station method. *Geophys. J.R. astr. Soc.*, **78**: 573-617.
- NAKANISHI, I. & ANDERSON, D.L. - 1984b - Aspherical heterogeneity of the mantle from phase velocities of mantle waves. *Nature*, **307**: 117-121.
- NAKANISHI, I. & KANAMORI, H. - 1982 - Effects of lateral heterogeneity and source process time on the linear moment tensor inversion of long-period Rayleigh waves. *Bull. Seismol. Soc. Am.*, **72**: 2063-2080.
- NISHIMURA, C.E. & FORSYTH, D.W. - 1985 - Anomalous Love-wave phase velocities in the Pacific: sequential pure-path and spherical harmonic inversion. *Geophys. J.R. astr. Soc.*, **81**: 389-407.
- PATTON, H.J. - 1978 - Source and propagation effects of Rayleigh waves from central Asian earthquakes. PhD Thesis, Mass. Inst. of Tech., Cambridge, 342 pp.
- PATTON, H.J. - 1980 - Reference point equalization method for determining the source and path effects of surface waves. *J. Geophys. Res.*, **85**: 821-848.
- PATTON, H.J. - 1984 - Regionalization of surface wave phase velocities in the western United States. *Earthquake Notes*, **55**: 23-24.
- PILANT, W.L. - 1967 - Tectonic features of the Earth's crust and upper mantle. Final Technical Report, AFOSR 67 - 1797, Air Force Off. Sci. Res., Aug.
- RAIKES, S.A. - 1980 - Regional variations in upper mantle structure beneath southern California. *Geophys. J.R. astr. Soc.*, **63**: 187-216.
- ROMANOWICZ, B.A. - 1982a - Moment tensor inversion of long period Rayleigh waves: a new approach. *J. Geophys. Res.*, **87**: 5394-5407.
- ROMANOWICZ, B.A. - 1982b - Lateral heterogeneity in continents: moment-tensor inversion of long-period surface waves and depth resolution of crustal events; body-wave modelling and phase-velocity calibrations. *Phys. Earth Planet. Inter.*, **30**: 269-271.
- ROSA, J.W.C. - 1986 - A global study on phase velocity, group velocity and attenuation of Rayleigh waves in the period range 20 to 100 seconds. PhD Thesis, Mass. Inst. of Technol., Cambridge, 859 pp.
- ROSA, J.W.C. & AKI, K. - 1991 - Global compilation of phase and group velocities of fundamental mode Rayleigh waves in the period range 20 to 100 sec. (This volume).
- SANTO, T.A. - 1960a - Observation of surface waves by Columbia-type seismograph installed at Tsukuba Station, Japan. Part I: Rayleigh wave dispersions across the oceanic basin. *Bull. Earthq. Res. Inst.*, **38**: 219-240.
- SANTO, T.A. - 1960b - Rayleigh wave dispersions across the oceanic basin around Japan. Part II. *Bull. Earthq. Res. Inst.*, **38**: 385-401.
- SANTO, T.A. - 1961a - Rayleigh wave dispersions across the oceanic basin around Japan. Part III: On the crust of

- the south-western Pacific Ocean. *Bull. Earthq. Res. Inst.*, **39**: 1-22.
- SANTO, T.A. - 1961b - Division of the south-western Pacific area into several regions in each of which Rayleigh waves have the same dispersion characters. *Bull. Earthq. Res. Inst.*, **39**: 603-630.
- SANTO, T.A. - 1963 - Division of the Pacific area into seven regions in each of which Rayleigh waves have the same group velocities. *Bull. Earthq. Res. Inst.*, **41**: 719-741.
- SANTO, T.A. - 1965a - Lateral variation of Rayleigh wave dispersion character. Part I: Observacional data. *Pure and Applied Geophysics*, **62**: 49-66.
- SANTO, T.A. - 1965b - Lateral variation of Rayleigh wave dispersion character. Part II: Eurasia. *Pure and Applied Geophysics*, **62**: 67-80.
- SANTO, T.A. - 1966 - Lateral variation of Rayleigh wave dispersion character. Part III: Atlantic Ocean, Africa and India Ocean. *Pure and Applied Geophysics*, **63**: 40-59.
- SANTO, T.A. - 1967 - Lateral variation of Rayleigh wave dispersion character. Part IV: The Gulf of Mexico and Caribbean Sea. *Bull. Earthq. Res. Inst.*, **45**: 963-971.
- SANTO, T.A. - 1968 - Lateral variation of Rayleigh wave dispersion character. Part V: North American Continent and Arctic Ocean. *Bull. Earthq. Res. Inst.*, **46**: 431-456.
- SANTO, T.A. & SATO, Y. - 1966 - World-wide survey of the regional characteristics of group velocity dispersion of Rayleigh waves. *Bull. Earthq. Res. Inst.*, **44**: 939-964.
- SATO, Y. & SANTO, T.A. - 1969 - World-wide distribution of the group velocity of Rayleigh wave as determined by dispersion data. *Bull. Earthq. Res. Inst.*, **47**: 31-41.
- SAVAGE, J.C. & WHITE, W.R.H. - 1969 - A map of Rayleigh-wave dispersion in the Pacific. *Canadian J. Earth Sci.*, **6**: 1289-1300.
- SORIAU-THEVENARD, A. - 1976 - Structure of the crust and the upper mantle in the southwest of France, from surface waves. *Ann. Geophys.*, **32**: 63-69.
- STRANG, G. - 1980 - Linear algebra and its applications. Second edition, Academic Press, New York.
- TANIMOTO, T. - 1985 - The Backus-Gilbert approach to the three-dimensional structure in the upper mantle. I. Lateral variation of surface wave phase velocity with its error and resolution. *Geophys. J.R. astr. Soc.*, **82**: 105-123.
- TANIMOTO, T. & ANDERSON, D.L. - 1984 - Mapping convection in the mantle. *Geophys. Res. Lett.*, **11**: 287-290.
- TANIMOTO, T. & ANDERSON, D.L. - 1985 - Lateral heterogeneity and azimuthal anisotropy of the upper mantle: Love and Rayleigh waves 100-250 sec. *J. Geophys. Res.*, **90**: 1842-1858.
- TARANTOLA, A. & VALETTE, B. - 1982 - Generalized nonlinear inverse problems solved using the least squares criterion. *Rev. Geophys. Space Phy.*, **20**: 219-232.
- TARR, A.C. - 1969 - Rayleigh-wave dispersion in the North Atlantic Ocean, Caribbean Sea and Gulf of Mexico. *J. Geophys. Res.*, **74**: 1591-1607.
- TAYLOR, S.R. - 1983 - Three-dimensional crust and upper mantle structure at the Nevada Test Site. *J. Geophys. Res.*, **88**: 2220-2232.
- WEIDNER, D.J. - 1972 - Rayleigh waves from mid-ocean ridge earthquakes: source and path effects. PhD Thesis, Mass. Inst. Technol., Cambridge, 256 pp.
- WEIDNER, D.J. & AKI, K. - 1973 - Focal depth and mechanism of mid-ocean ridge earthquakes. *J. Geophys. Res.*, **78**: 1818-1831.
- WOODHOUSE, J.H. & DZIEWONSKI, A.M. - 1984 - Mapping the upper mantle: three-dimensional modelling of Earth structure by inversion of seismic waveforms. *J. Geophys. Res.*, **89**: 5953-5986.
- YOMOGIDA, K. - 1985 - Amplitude and phase variations of surface waves in a laterally heterogeneous Earth: ray- and beam-theoretical approach. PhD Thesis, Mass. Inst. Technol., Cambridge, 227 pp.
- YOSHII, T. - 1975 - Regionality of group velocities of Rayleigh waves in the Pacific and thickening of the plate. *Earth Planet. Sci. Lett.*, **25**: 305-312.
- YU, G. & MITCHELL, B.J. - 1979 - Regionalized shear velocity models of the Pacific upper mantle from observed Love and Rayleigh wave dispersion. *Geophys. J.R. astr. Soc.*, **57**: 311-341.
- ZANDT, G. - 1978 - Study of three-dimensional heterogeneity beneath seismic arrays in central California and Yellowstone, Wyoming. PhD Thesis, Mass. Inst. Technol., Cambridge, 490 pp.

Versão recebida em: 15/05/90

Versão revista e aceita em: 29/11/90

Editor Associado: M.S. Assumpção